

AD-A150 813

HIGNER DISTRIBUTION FUNCTION AS A LOFARGRAM WITH  
UNLIMITED RESOLUTION SIMULTANEOUSLY IN TIME AND  
FREQUENCY(U) MITRE CORP MCLEAN VA W PRESS AUG 83

1/1

UNCLASSIFIED

JSR-83-212 F19628-84-C-0001

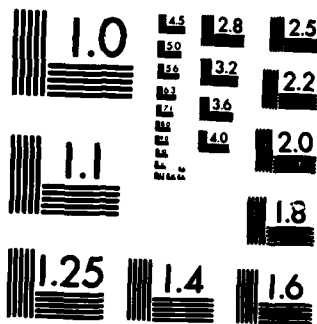
F/G 17/1

NL

END

FILED

DTIC



MICROCOPY RESOLUTION TEST CHART  
NATIONAL BUREAU OF STANDARDS-1963-A

2

AD-A150 813

# Wigner Distribution Function as a LOFARGRAM with Unlimited Resolution Simultaneously in Time and Frequency

FILE COPY

ALL INFORMATION CONTAINED  
HEREIN IS UNCLASSIFIED  
DATE 08-13-2001 BY 60322

MITRE

85 02 13 2001

DTIC  
SELECTE  
MAR 01 1985  
E

---

# Wigner Distribution Function as a LOFARGRAM with Unlimited Resolution Simultaneously in Time and Frequency

---

William Press

January 1985

ISR-83-212

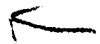
Approved for public release; distribution unlimited.

*DAR PA  
Contract No. F19628-84-C-0001*

JASON  
The MITRE Corporation  
1820 Dolley Madison Boulevard  
McLean, Virginia 22102

Unclassified

SECURITY CLASSIFICATION OF THIS PAGE (When Data Entered)

REPORT DOCUMENTATION PAGE		READ INSTRUCTIONS BEFORE COMPLETING FORM	
1. REPORT NUMBER JSR-83-212	2. GOVT ACCESSION NO.	3. RECIPIENT'S CATALOG NUMBER	
4. TITLE (and Subtitle)  Wigner Distribution Function as a Lofargram With Unlimited Resolution Simultaneously in Time and Frequency		5. TYPE OF REPORT & PERIOD COVERED	
		6. PERFORMING ORG. REPORT NUMBER	
7. AUTHOR(s)  William Press		8. CONTRACT OR GRANT NUMBER(s)  F19628-84-C-0001	
9. PERFORMING ORGANIZATION NAME AND ADDRESS  The MITRE Corporation 1820 Dolley Madison Boulevard McLean, Virginia 22102		10. PROGRAM ELEMENT, PROJECT, TASK AREA & WORK UNIT NUMBERS	
11. CONTROLLING OFFICE NAME AND ADDRESS		12. REPORT DATE Aug 1983	13. NO. OF PAGES 23
		15. SECURITY CLASS. (of this report)  Unclassified	
14. MONITORING AGENCY NAME & ADDRESS (if diff. from Controlling Office)		15a. DECLASSIFICATION/DOWNGRADING SCHEDULE	
16. DISTRIBUTION STATEMENT (of this report)			
17. DISTRIBUTION STATEMENT (of the abstract entered in Block 20, if different from report)			
18. SUPPLEMENTARY NOTES			
19. KEY WORDS (Continue on reverse side if necessary and identify by block number)  Sonar, Lofargram, Wigner Distribution Function. 			
20. ABSTRACT (Continue on reverse side if necessary and identify by block number)  The purpose of this note is to provide a pedagogical introduction to the so-called "Wigner distribution function", and to demonstrate that what is generally known is not necessarily correct: the Wigner distribution function displays a signal as a function of both frequency and time, but in a manner that is not resolution limited in either domain. We think it possible that the Wigner distribution can be used to provide a graphic realization of passive sonar signals that is sufficiently close in character to conventional lofargrams so that their body of accumulated wisdom will still be applicable, yet provide significant new detailed information on the sonar signal.			

DD FORM 1473

1 JAN 73  
EDITION OF 1 NOV 65 IS OBSOLETE

Unclassified

SECURITY CLASSIFICATION OF THIS PAGE (When Data Entered)

# TABLE OF CONTENTS

	<u>PAGE</u>
1.0 INTRODUCTION.....	1
2.0 FOURIER TRANSFORM OF THE SPECTROGRAM PLANE.....	3
3.0 WIGNER DISTRIBUTION FUNCTION.....	7
4.0 EXAMPLES.....	9
4.1 Segment of Pure Tone.....	9
4.2 Periodic Series of Clicks.....	14
5.0 DISCUSSION.....	17
REFERENCES.....	20
DISTRIBUTION LIST.....	D-1

Accession For	
NTIS GRA&I	<input checked="" type="checkbox"/>
DTIC TAB	<input type="checkbox"/>
Unannounced	<input type="checkbox"/>
Justification	
By _____	
Distribution/	
Availability Codes	
Dist	Avail and/or Special
A-1	



## 1.0 INTRODUCTION

One is familiar with the display of a passive sonar signal as a lofargram, where the "instantaneous" spectrum is displayed horizontally as a function of time running vertically downward. Of course, there is actually no such thing as an instantaneous spectrum; rather, the spectrum is determined for a time interval  $\Delta t$ , either by taking the discrete Fourier transform of the signal sampled during that time interval at the appropriate Nyquist rate, or else by analog means using narrowband filters.

Also generally known is that the frequency resolution of the spectrum,  $\Delta f$ , is not independently specifiable, but rather varies inversely to the time interval according to (what physicists call) the uncertainty principle,

$$\Delta t \Delta f = 1 \quad . \quad (1.1)$$

Thus, one can choose to have either lofargrams with fine time resolution and poor frequency resolution (obtained using short coherent integration times) or else, vice versa, with fine frequency resolution and poor time resolution (obtained using long coherent integration times).

The purpose of this note is to provide a pedagogical introduction to the so-called "Wigner distribution function"<sup>[1]</sup>, and to demonstrate that what is generally known is not necessarily correct: the Wigner distribution function displays a signal as a function of both frequency and time, but in a manner that is not resolution limited in either domain. We think it possible that the Wigner distribution can be used to provide a graphic realization of passive sonar signals that is sufficiently close in character to conventional lofargrams so that their body of accumulated wisdom will still be applicable, yet provide significant new detailed information on the sonar signal.

Originally invented by Wigner and Szilard<sup>[1]</sup> for applications in quantum statistical mechanics (see, e.g., [2]), the Wigner distribution has surfaced from time to time in fluid dynamical applications (e.g., [3]), in optical signal processing [4,5], and for the analysis of speech [8]. As we will see, it is closely related to, but different from, some standard concepts in radar processing [6].



## 2.0 FOURIER TRANSFORM OF THE SPECTROGRAM PLANE

We can define the lofargram of a signal  $s(t)$  as follows:  
Centered around a given time  $t_0$ , multiply the signal by a  
localized window function  $w(t - t_0)$ , then Fourier transform the  
result. We obtain a function of both frequency  $f$  and time  $t_0$ .

$$S(f, t_0) = \left| \int dt e^{2\pi i f t} s(t) w(t - t_0) \right|^2. \quad (2.1)$$

The window function  $w$  is frequently taken to be a square window of  
some width  $\tau$ , equivalent to taking a uniform sample of the  
signal. Alternatively, the window might be a Gaussian of width  
 $\tau$ . We will assume this latter case as a mathematical  
convenience.

Something interesting will emerge if we take the two-  
dimensional Fourier transform of (2.1)

$$\begin{aligned} R(\lambda, \mu) &= \int dt_0 e^{2\pi i \lambda t_0} \int df e^{2\pi i \mu f} S(f, t_0) \\ &= \iiint dt_0 df dt dt' e^{2\pi i \lambda t_0} e^{2\pi i \mu f} \frac{e^{2\pi i f t} e^{-2\pi i f t'}}{e} \\ &\quad s(t) s(t') w(t - t_0) w(t' - t_0). \end{aligned} \quad (2.2)$$

The second line of (2.2) follows from writing out the modulus square of (2.1) as the product of the integral with its complex conjugate. The signal  $s(t)$  is assumed to be real.

The integrals over  $f$  and  $t'$  in (2.2) can be done, giving in turn

$$\begin{aligned} R(\lambda, \mu) &= \iiint dt_0 dt dt' \delta(\mu+t-t') e^{2\pi i \lambda t_0} s(t) s(t') w(t-t_0) w(t'-t_0) \\ &= \int dt s(t) s(t+\mu) \int dt_0 e^{2\pi i \lambda t_0} w(t-t_0) w(t+\mu-t_0) \end{aligned} \quad (2.3)$$

Now notice that the second integral in the second line of (2.3) depends only on the window function, not on the signal. For a Gaussian window

$$w(x) = e^{-x^2/(2\tau^2)} \quad (2.4)$$

the integral can be done analytically, giving

$$R(\lambda, \mu) = e^{-\mu^2/(4\tau^2)} e^{-(\lambda\tau)^2/4} \int dt s\left(t - \frac{\mu}{2}\right) s\left(t + \frac{\mu}{2}\right) e^{2\pi i \lambda t} \quad (2.5)$$

In (2.5) we have also redefined the dummy variable  $t$  so as to make the integrand more symmetrical.

Notice that the width  $\tau$  of the window function appears only in the exponentials in front of the integral, and that the integral is a functional only of the signal  $s(t)$  and of the parameters  $\lambda$  and  $\mu$ . If we make  $\tau$  very large, then the exponentials in front cut off very rapidly in  $\lambda$ , but only very slowly in  $\mu$ . If we make  $\tau$  very small, the reverse is true. In general, the only function of the exponentials in front of the integral is to "enforce" the uncertainty principle in the 2-dimensional Fourier domain: the lofargram cannot simultaneously contain rapidly varying information in the  $f$  (conjugate variable  $\mu$ ) and  $t_0$  (conjugate variable  $\lambda$ ) directions.

But why not simply strip off the exponentials that enforce the uncertainty principle and examine the remaining piece, which depends only on the signal,

$$Q(\lambda, \mu) \equiv \int dt \, s\left(t - \frac{\mu}{2}\right) s\left(t + \frac{\mu}{2}\right) e^{2\pi i \lambda t} . \quad (2.6)$$

In fact, this object has a conventional name; it is the symmetrical autoambiguity function of the signal (see Ref. 6). So the (purely pedagogical) result of this section is: the autoambiguity function of a signal is the (window-independent piece of the) 2-dimensional Fourier transform of its lofargram.

### 3.0 WIGNER DISTRIBUTION FUNCTION

Now we do the obvious thing. We take inverse Fourier transforms to get back to the 2-dimensional lofargram space. We will not get back our original lofargram, because we have stripped off the dependence on the window function. We want to emphasize that this is not the same as taking any particular window (e.g., very wide or very narrow); it corresponds instead to taking no window at all!

$$\begin{aligned} P(f, t_0) &\equiv \int e^{-2\pi i t_0 \lambda} d\lambda \int e^{-2\pi i f \mu} d\mu Q(\lambda, \mu) \\ &= \int d\mu s\left(t_0 - \frac{\mu}{2}\right) s\left(t_0 + \frac{\mu}{2}\right) e^{2\pi i f \mu} . \end{aligned} \tag{3.1}$$

This is the Wigner distribution function of the signal  $s(t)$ . It is a function of both time and frequency, just like the lofargram. The second line of (3.1) is obtained by doing the integral over  $\lambda$  in the first line.

An interesting identity is that the Wigner distribution  $P(f, t_0)$  can also be expressed in terms of the Fourier transform  $S(f)$  of the signal  $s(t)$

$$P(f, t_0) = \int S^* \left( f - \frac{\lambda}{2} \right) S \left( f + \frac{\lambda}{2} \right) e^{-2\pi i \lambda t_0} d\lambda . \quad (3.2)$$

We see that the Wigner distribution function is quadratic in the signal amplitude, just like the lofargram (2.1). It is not, however, positive definite. We will see why this is so in section 4.

It is worth noting that the computation of the Wigner distribution is not significantly slower than the computation of the lofargram (2.1), which requires one Fourier transform (FFT) for each time  $t_0$  of interest. The Wigner distribution (3.1) also requires one FFT for each value of  $t_0$ . The series of points that is FFT'd is, however, not the windowed signal, but is rather the symmetrical product of the signal at positive and negative lags.

References [4] and [5] prove many theorems about the Wigner distribution, and give further references. We will not repeat that material here. Rather, in the next section, we will sketch a couple of simple analytic examples which give some insight into what one might actually "see" in the Wigner distribution of a passive sonar signal.

#### 4.0 EXAMPLES

##### 4.1 Segment of Pure Tone

Suppose the input signal is

$$\begin{aligned} s(t) &= \cos(\omega t) & -\frac{\tau}{2} < t < \frac{\tau}{2} \\ &= 0 & \text{otherwise} \end{aligned} \quad (4.1)$$

Then the Wigner distribution  $P(f, t_0)$  is evidently zero outside of the interval  $-\frac{\tau}{2} < t_0 < \frac{\tau}{2}$ , since in the integral (3.1) one or the other of the two terms in  $s(t \pm \frac{\mu}{2})$  will be zero. So, we see that the Wigner distribution turns on instantaneously with the signal.

In the interval  $-\frac{\tau}{2} < t_0 < \frac{\tau}{2}$  where it is nonzero,  $P(f, t_0)$  is symmetric around  $t = 0$ , so without loss of generality we can confine attention to the case of  $0 < t_0 < \frac{\tau}{2}$ . In this case  $\mu$  ranges from  $-(\frac{\tau}{2} - t_0)$  to  $+(\frac{\tau}{2} - t_0)$ . Using trigonometric identities, (3.1) can be rewritten as

$$\begin{aligned}
P(f, t_0) &= \frac{1}{2} \int_{-\frac{\tau}{2} - t_0}^{\frac{\tau}{2} - t_0} d\mu \cos(2\pi f\mu) [\cos(2\omega t_0) + \cos(\omega\mu)] \\
&= \cos(2\omega t_0) \frac{\sin[2\pi f(\frac{\tau}{2} - t_0)]}{2\pi f} \\
&\quad + \frac{1}{2} \frac{\sin[(\omega + 2\pi f)(\frac{\tau}{2} - t_0)]}{\omega + 2\pi f} + \frac{\sin[(\omega - 2\pi f)(\frac{\tau}{2} - t_0)]}{\omega - 2\pi f} \quad (4.2)
\end{aligned}$$

Notice that (4.2) is the sum of three resonance integrals. Each has a main-lobe width in the frequency direction of about  $1/\tau$ . In other words, the longer the duration of the tone, the narrower the frequency resolution reflected in the Wigner distribution. This is just as we would expect it to be, with the novel feature that there is no need for us to search for the "best" integration time for the signal: the Wigner distribution does this for us automatically.

Where, in the frequency direction, are the three resonances? Two are at  $f = \pm \omega/2\pi$ , where we would expect them to be. The third is at  $f = 0$ . To understand this one, we need to examine the dependence of the three resonances on time  $t_0$ . The dependence on  $t_0$  inside the resonance terms just gives all three resonances a kind of broadening as the boundary in time is



approached. More important is the rapidly oscillating term, with angular frequency twice that of the signal, which multiplies the zero-frequency resonance term. Figure 1 sketches the location and sign of the main-lobe peaks or ridges of equation (4.2).

To understand what is going on in the figure, imagine that the figure is averaged or smeared in the horizontal direction. Then the amplitudes at zero frequency average to zero, and one will be left with narrow frequency resonances at  $f = \pm \omega/2\pi$  which are smeared out in time. This is precisely the lofargram of the signal if constructed with a wide time-window: it maintains frequency resolution but smears out time resolution. By contrast, next imagine that the figure is averaged or smeared in the vertical direction. Then the zero-frequency positive peaks reinforce the positive values at  $f = \pm \omega/2\pi$  to give vertical smears located at the positive and negative peaks of the original signal, while the zero-frequency negative peaks exactly cancel with the positive values at  $f = \pm \omega/2\pi$  to give zero response at the zeros of the original signal. This is exactly the lofargram of the signal if constructed with a narrow time-window.

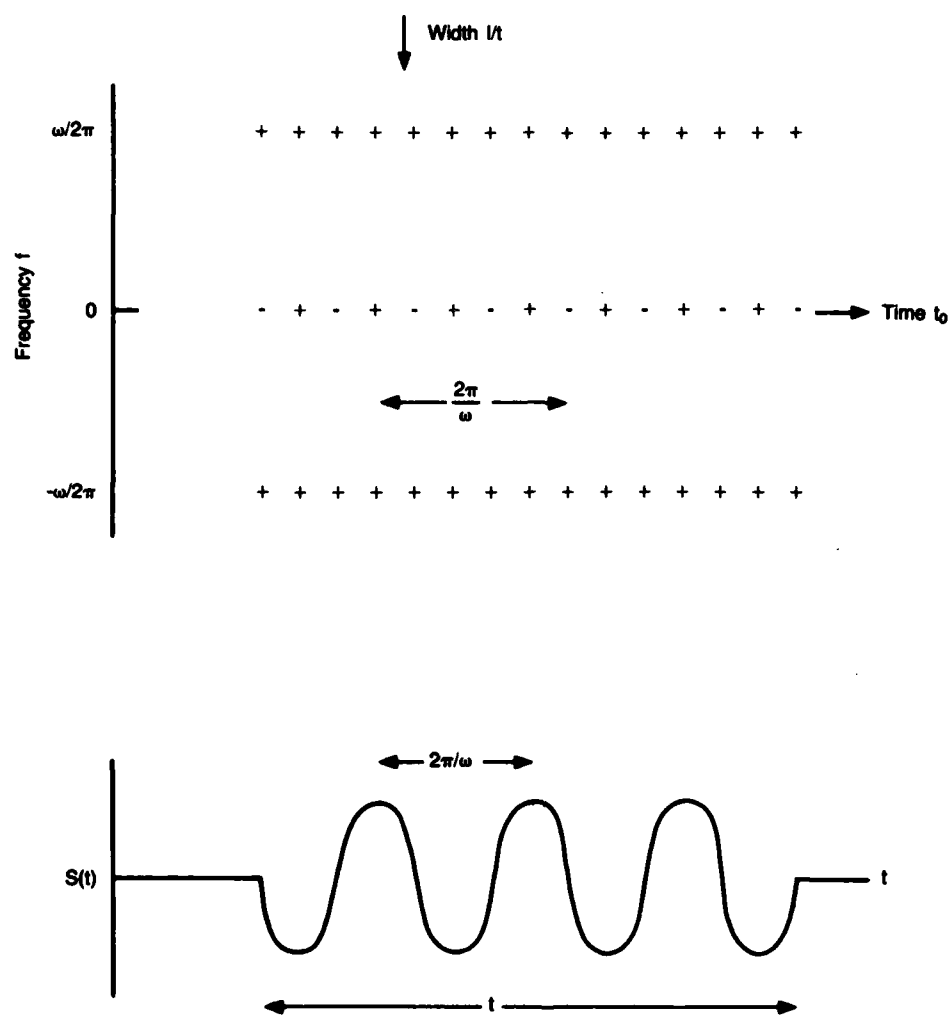


Figure 1. Wigner distribution of the signal (4.1)

So, in summary, we see that the Wigner distribution displays simultaneously all the structures which would emerge from lofargram with any window width, or (for that matter) with any window shape.

## 4.2 Periodic Series of Clicks

We can see the same general ideas emerging in another example. Consider the signal

$$s(t) = \sum_{n=-\infty}^{+\infty} \delta(t - nT) \quad (4.3)$$

This represents a sequence of sharp clicks (delta functions), equally spaced with period  $T$ . The Wigner distribution is thus

$$\begin{aligned} & \int d\mu \sum_n s(t_0 - \frac{\mu}{2} - nT) \delta(t_0 + \frac{\mu}{2} - nT) e^{2\pi i f \mu} \\ &= \sum_n e^{2\pi i f (2nT)} \quad \text{for } t_0 = \dots -2T, -T, 0, T, 2T \dots \\ & \quad \sum_n e^{2\pi i f (2n+1)T} \quad \text{for } t_0 = \dots -\frac{3}{2}T, -\frac{1}{2}T, \frac{1}{2}T, \frac{3}{2}T \dots \\ &= \sum_k \sum_l \delta(t_0 - kT) \delta(f - \frac{l}{2T}) + (-1)^l \delta(t_0 - [k + \frac{1}{2}]T) \delta(f - \frac{l}{2T}) \end{aligned} \quad (4.4)$$

(except for a normalizing constant). Figure 2 shows the locations and signs of the delta-function peaks out of which this Wigner distribution is composed.

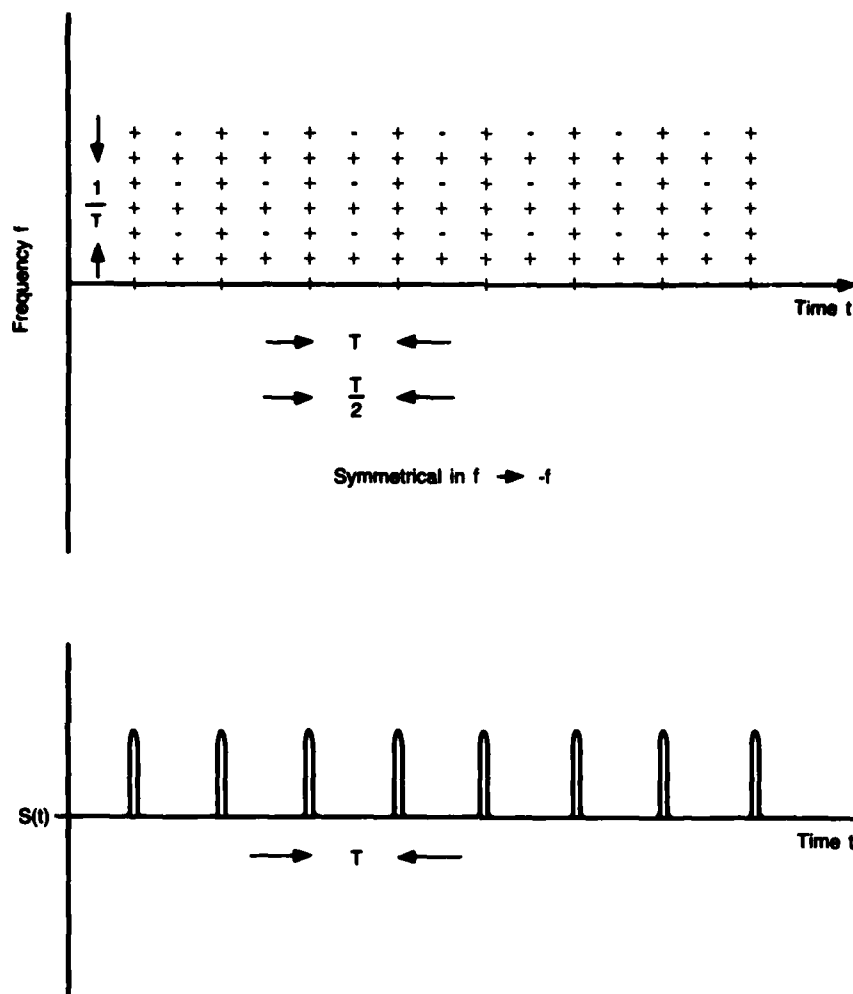


Figure 2. Wigner distribution of the signal (4.3).

Notice that the positive delta functions form two interlocking sets of lines, horizontal and vertical. In the centers of the lattice thus formed are the isolated negative delta functions. The vertical lines of positive delta functions are separated in time by  $T$ , and they represent the signal with infinitely good time resolution. The horizontal lines of delta functions are separated in frequency by a spacing of  $1/T$ , and they represent the fundamental and higher harmonics of the signal (which is, after all, perfectly periodic) with infinitely good frequency resolution.

So what function do the negative delta functions perform? The answer can be seen by again imagining that the Wigner function is smeared either horizontally or vertically. In that case, the negative values cancel out either the power between the perfect harmonic rows, or the power between the perfectly time-resolved pulses, in both cases giving realizable lofargrams.

In fact, one can see intuitively that any smearing of Figure 2 that obeys the uncertainty principle will give a positive-definite lofargram: Since each minus sign is surrounded by eight plus signs, there is no way to center a window of unit area on the minus sign without bringing in more than enough plus signs to give positivity. It is generally true on Wigner distributions that

negative values are in close proximity to positive values both in the frequency and time directions--so that any realizable lofargram can come out positive-definite as it must.

## 5.0 DISCUSSION

It may require some experimentation to discover the best graphical display of a Wigner distribution function. We have not yet done this experimentation, but intend to do so in the near future. One desires a format in which the information is presented in a manner as close as possible to that of the standard lofargram.

One good candidate for a display format is a grey-scale presentation ranging from the most negative values (pure white) to most positive (pure black). In this format, regions where negative and positive lobes are in close proximity will have a mid-scale grey tone, while positive features will appear as darker lines or regions. The human eye is quite good at picking out linear black features in a noisy grey-scale background, so that details of high resolution simultaneously in frequency and time may be readily apparent.

Other display formats are also under consideration and will be tried in due course.

Although we do not yet have actual data, we have reason to hope for a graphical presentation in which unrelated signals will



appear with distinguishable natural line widths, so the discrimination between submarine and surface-ship signatures is aided. Also, we would hope that the detectability of very weak but very narrow lines will be furthered, if they appear "automatically" in a display, without the necessity of special narrowband processing. Finally, when high-resolution frequency and high-resolution time information is displayed simultaneously, there may be serendipitous features in the signal which would not otherwise be noted, and which may yield new discrimination techniques.

#### REFERENCES

1. Wigner, E. Phys. Rev. 40, 749 (1932).
2. Snider, R.F. J. Chem. Phys. 32, 1051 (1960).
3. Watson, K.M. and West, B.J. J. Fluid Mech. 70, 815 (1975).
4. Bastiaans, M.J. Optics Communications 30, 321 (1979).
5. Bastiaans, M.J. Optica Acta 28, 1215 (1981).
6. Skolnik, M.I. Radar Handbook (McGraw Hill, 1970) p. 3-35.
7. Fant, Gunnar Acoustic Theory of Speech Production (Mouton, 1970).
8. Gerzon, Michael A. J. Audio Eng. Soc. 22, 104 (1974).

DISTRIBUTION LIST

Dr. Marv Atkins  
Deputy Director, Science & Tech.  
Defense Nuclear Agency  
Washington, D.C. 20305

National Security Agency  
Attn RS: Dr. N. Addison Ball  
Ft. George G. Meade, MD 20755

Dr. Robert Cooper [2]  
Director, DARPA  
1400 Wilson Boulevard  
Arlington, VA 22209

Defense Technical Information [2]  
Center  
Cameron Station  
Alexandria, VA 22314

The Honorable Richard DeLauer  
Under Secretary of Defense (R&E)  
Office of the Secretary of  
Defense  
The Pentagon, Room 3E1006  
Washington, D.C. 20301

Director [2]  
National Security Agency  
Fort Meade, MD 20755  
ATTN: Mr. Richard Foss, A05

CAPT Craig E. Dorman  
Department of the Navy, OP-095T  
The Pentagon, Room 5D576  
Washington, D.C. 20350

CDR Timothy Dugan  
NFOIO Detachment, Suitland  
4301 Suitland Road  
Washington, D.C. 20390

Dr. Larry Gershwin  
NIO for Strategic Programs  
P.O. Box 1925  
Washington, D.C. 20505

Dr. S. William Gouse, W300  
Vice President and General  
Manager  
The MITRE Corporation  
1820 Dolley Madison Blvd.  
McLean, VA 22102

Dr. Edward Harper  
SSBN, Security Director  
OP-021T  
The Pentagon, Room 4D534  
Washington, D.C. 20350

Mr. R. Evan Hineman  
Deputy Director for Science  
& Technology  
P.O. Box 1925  
Washington, D.C. 20505

Mr. Ben Hunter [2]  
CIA/DDS&T  
P.O. Box 1925  
Washington, D.C. 20505

The MITRE Corporation [25]  
1820 Dolley Madison Blvd.  
McLean, VA 22102  
ATTN: JASON Library, W002

Mr. Jack Kalish  
Deputy Program Manager  
The Pentagon  
Washington, D.C. 20301

Mr. John F. Kaufmann  
Dep. Dir. for Program Analysis  
Office of Energy Research, ER-31  
Room F326  
U.S. Department of Energy  
Washington, D.C. 20545

DISTRIBUTION LIST (Cont'd.)

Dr. George A. Keyworth  
Director  
Office of Science & Tech. Policy  
Old Executive Office Building  
17th & Pennsylvania, N.W.  
Washington, D.C. 20500

MAJ GEN Donald L. Lamberson  
Assistant Deputy Chief of Staff  
(RD&A) HQ USAF/RD  
Washington, D.C. 20330

Dr. Donald M. LeVine, W385 [3]  
The MITRE Corporation  
1820 Dolley Madison Blvd.  
McLean, VA 22102

Mr. V. Larry Lynn  
Deputy Director, DARPA  
1400 Wilson Boulevard  
Arlington, VA 22209

Dr. Joseph Mangano [2]  
DARPA/DEO  
9th floor, Directed Energy Office  
1400 Wilson Boulevard  
Arlington, VA 22209

Mr. John McMahon  
Dep. Dir. Cen. Intelligence  
P.O. Box 1925  
Washington, D.C. 20505

Director  
National Security Agency  
Fort Meade, MD 20755  
ATTN: William Mehuron, DDR

Dr. Marvin Moss  
Technical Director  
Office of Naval Research  
800 N. Quincy Street  
Arlington, VA 22217

Dr. Julian Nall [2]  
P.O. Box 1925  
Washington, D.C. 20505

Director  
National Security Agency  
Fort Meade, MD 20755  
ATTN: Mr. Edward P. Neuburg  
DDR-FANX 3

Prof. William A. Nierenberg  
Scripps Institution of  
Oceanography  
University of California, S.D.  
La Jolla, CA 92093

Mr. C. Wayne Peale  
Office of Research and  
Development  
P.O. Box 1925  
Washington, DC 20505

The MITRE Corporation  
Records Resources  
Mail Stop W971  
McLean, VA 22102

Mr. Alan J. Roberts  
Vice President & General Manager  
Washington C<sup>3</sup> Operations  
The MITRE Corporation  
1820 Dolley Madison Boulevard  
McLean, VA 22102

Los Alamos Scientific Laboratory  
ATTN: C. Paul Robinson  
P.O. Box 1000  
Los Alamos, NM 87545

Mr. Richard Ross [2]  
P.O. Box 1925  
Washington, D.C. 20505

DISTRIBUTION LIST (Concl'd.)

Dr. Phil Selwyn  
Technical Director  
Office of Naval Technology  
800 N. Quincy Street  
Arlington, VA 22217

Mr. Leo Young  
OUSDRE (R&AT)  
The Pentagon, Room 3D1067  
Washington, D.C. 20301

Dr. Eugene Sevin [2]  
Defense Nuclear Agency  
Washington, D.C. 20305

Mr. Robert Shuckman  
P.O. Box 8618  
Ann Arbor, MI 48107

Dr. Joel A. Snow [2]  
Senior Technical Advisor  
Office of Energy Research  
U.S. DOE, M.S. E084  
Washington, D.C. 20585

Mr. Alexander J. Tachmindji  
Senior Vice President & General  
Manager  
The MITRE Corporation  
P.O. Box 208  
Bedford, MA 01730

Dr. Vigdor Teplitz  
ACDA  
320 21st Street, N.W.  
Room 4484  
Washington, D.C. 20451

Dr. Al Trivelpiece  
Director, Office of Energy  
Research, U.S. DOE  
M.S. 6E084  
Washington, D.C. 20585

Mr. James P. Wade, Jr.  
Prin. Dep. Under Secretary of  
Defense for R&E  
The Pentagon, Room 3E1014  
Washington, D.C. 20301

**END**

**FILMED**

**4-85**

**DTIC**